

PACS numbers: 52.38.-r; 52.50.Jm
DOI: 10.1070/QE2006v036n05ABEH013242

Efficiency of ablative loading of material upon the fast-electron transfer of absorbed laser energy

S.Yu. Gus'kov, A. Kasperczuk, T. Pisarczyk, S. Borodziuk, M. Kalal, J. Limpouch, J. Ullschmied, E. Krousky, K. Masek, M. Pfeifer, K. Rohlena, J. Skala, P. Pisarczyk

***Abstract*. We present the results of experiments on the short-term irradiation of a solid material by a laser beam. The data testify to a rise in efficiency of the energy transfer from the laser pulse to a shock wave due to the fast-electron energy transfer. The experiments were performed with massive aluminium targets on the PALS iodine laser, whose pulse duration (0.4 ns) was much shorter than the time of shock decay and crater formation in the target (50 – 200 ns). The irradiation experiments were carried out using the fundamental laser harmonic (1.315 μm) with an energy of 360 J. The greater part of the experiments were performed for the radiation intensity exceeding 10^{15} W cm^{-2}, which corresponded to the efficient generation of fast electrons under the conditions where the relatively long-wavelength iodine-laser radiation was employed. The irradiation intensity was varied by varying the laser beam radius for a specified pulse energy.**

Keywords: *ablation, laser loading, fast electrons.*

1. Introduction

The aim of our work was to investigate the efficiency of energy transfer from the plasma-producing laser beam to a solid target under the conditions where the absorbed laser energy is converted to the energy of fast electrons. These investigations are a direct continuation of Ref. [1], where, apart from other results, a relation was established between the efficiency of laser-driven material loading (the fraction of laser pulse energy transferred to the shock wave propagating through a massive target) and the wavelength of laser radiation and its intensity in a wide range of these parameters.

The experimental conditions in Ref. [1] and the obtained data were as follows. The experiments were performed on the PALS iodine laser [2] and involved irradiation of massive aluminium targets by a laser pulse with an energy of 100 J and a FWHM duration of 0.4 ns. The targets thicknesses were much greater than the shock attenuation length. The laser radiation was focused onto the target with the aid of an aspheric lens with a focal distance of 593 mm. The targets were exposed to the first and third harmonics with the wavelengths $\lambda_1 = 1.315$ μm and $\lambda_3 = 0.438$ μm for the same energy of the laser pulse (100 J) for different irradiation intensities. The radiation intensity I at the target surface was varied in the range between 2×10^{13} and 7×10^{15} W cm^{-2} by varying the laser-beam radius upon changing the position of the focusing lens. The experiments were carried out for the beam radii $R_L = 35$, 100, 300, and 600 μm. The parameter $I\lambda^2$ was varied in the $4\times10^{12} - 1.3\times 10^{15}$ W μm^2 cm^{-2} range for the third harmonic radiation and in the $3.8 \times 10^{13} - 1.2\times 10^{16}$ W μm^2 cm^{-2} range for the first harmonic radiation.

The energy of the shock wave was determined by measuring the volume Ω of the crater produced on the target surface due to the action of a laser beam. The dependence of the efficiency of laser loading on the laser beam radius was determined. When the target was irradiated by the third harmonic, this dependence was rather smooth, while nonmonotonic, and was close to a parabolic dependence with a clearly defined maximum in the neighbourhood of the radius $R_L = 300$ μm. The efficiency of laser loading was 1.2×10^{-2} for $R_L = 600$ μm ($I = 2.2 \times 10^{13}$ W cm^{-2}), increased to 1.6×10^{-2} for $R_L = 300$ μm ($I = 8.8\times 10^{13}$ W cm^{-2}), and then lowered to 1.1×10^{-2} for $R_L =$ 100 μm ($I = 8.3 \times 10^{14}$ W cm^{-2}) and further to 0.65×10^{-2} for $R_L = 35$ μm ($I = 7.1 \times 10^{15}$ W cm^{-2}).

When the irradiation was performed by the first harmonic, the dependence of laser loading on the beam radius repeated the dependence for the third harmonic up to the radius $R_L = 100$ μm, although its maximum was less pronounced and its position was shifted towards longer radii. However, as the beam radius was further decreased (with increase in laser radiation intensity), the form of the dependence reversed in comparison with the dependence for the third harmonic; specifically, the fraction of transferred energy increased with decreasing the radius. The efficiency of laser loading for the first harmonic was equal to 0.5×10^{-2} for a radius $R_L = 600$ μm, rose to 0.58×10^{-2} for $R_L = 300$ μm, then decreased to 0.23×10^{-2} for

S.Yu. Gus'kov P.N. Lebedev Physics Institute, Russian Academy of Sciences, Leninsky prosp. 53, 119991 Moscow, Russia;
e-mail: guskov@sci.lebedev.ru;
A. Kasperczuk, T. Pisarczyk, S. Borodziuk Institute of Plasma Physics and Laser Microfusion, 23 Hery St., 00-908 Warsaw, Poland;
M. Kalal, J. Limpouch Czech Technical University in Prague, FNSPE, Brehova 7, 115 19 Prague 1, Czech Republic;
J. Ullschmied Institute of Plasma Physics AS CR, Za Slovankou 3, 182 00 Prague 8, Czech Republic;
E. Krousky, K. Masek, M. Pfeifer, K. Rohlena, J. Skala Institute of Physics Acad. Sci. CR, Na Slovance 2, 182 21 Prague 8, Czech Republic;
P. Pisarczyk Warsaw University of Technology, ICS, 15/19 Nowowiejska St., 00-665 Warsaw, Poland

Received 6 December 2005
Kvantovaya Elektronika **36** (5) 429 – 434 (2006)
Translated by E.N. Ragozin

$R_L = 100$ μm and then increased again to 0.45×10^{-2} for $R_L = 35$ μm.

For equal radii of the laser beam (in the 600 – 100 μm range), the efficiency of laser loading for the third harmonic was 3 – 4 times higher than for the first one. However, for a radius $R_L = 35$ μm the efficiencies turned out to be approximately the same for both harmonics.

The experimental results described above were interpreted (including the numerical values of the parameters measured) on the basis of the analytical model, which was proposed in Ref. [1], describing the production and two-dimensional expansion of the plasma plume with the inclusion of two mechanisms for the absorption of laser radiation: 1) the inverse bremsstrahlung by thermal electrons – throughout the beam radius range in the case of experiments involving the third harmonic radiation as well as for long beam radii ($R_L = 600$ and 300 μm) in the case of experiments involving the first harmonic radiation, which correspond to moderate intensities; and 2) the resonance absorption for a total conversion of absorbed laser energy to the energy of fast electrons – in the case of experiments involving the first harmonic for small beam radii ($R_L < 100$ μm), which correspond to high intensities.

The laser loading efficiency of a target made of a material comprising light elements, in which it is possible to neglect the intrinsic radiative energy losses, is determined by the efficiency of two processes: the absorption of laser radiation in the vaporised part of the target (the plasma plume) and the transfer of energy from the plasma plume to the shock wave propagating through the non-vaporised part of the target. That is why the efficiency of laser loading is the product of two quantities: $\eta = K_{ab}\sigma$, where $K_{ab} = E_{ab}/E_L$ is the laser radiation absorption coefficient (E_L and E_{ab} are the energy of a laser pulse and its portion absorbed in the plasma plume) and $\sigma = E_{sw}/E_{ab}$ is the efficiency of ablative loading (E_{sw} is the energy of the shock wave).

The efficiency of ablative loading depends only on ratio between the plume density ρ_a at the ablation surface (the evaporation surface) and the density ρ_0 of the solid part of the target, with $\sigma \propto (\rho_a/\rho_0)^{1/2}$ under the conditions of laser ablation (when $\rho_a \ll \rho_0$) [3]. This general result follows directly from the condition for energy flux continuity at the ablation surface. Indeed, the flux of absorbed laser energy is proportional to the flux of thermal and kinetic energy at the ablation surface of the plume, $I_a \propto P_a \times (P_a/\rho_a)^{1/2}$ (P_a is the pressure at the ablation surface). The energy flux at the shock front in the solid part of the target is defined in terms of the pressure P_c at its front: $I_{sw} \propto P_c(P_c/\rho_0)^{1/2}$. Bearing in mind that $P_c \approx P_a$, correct to a constant factor which depends only on the adiabatic exponents in both parts of the target, we obtain $\sigma = I_{sw}/I_a \propto (\rho_a/\rho_0)^{1/2}$.

For $I\lambda^2$ parameter values not exceeding 10^{15} W μm^2 cm^{-2}, i.e. throughout the intensity range in the experiments involving the third harmonic, the dominant part is played by the inverse bremsstrahlung. In this case, the characteristic density of the radiation absorption region is the critical plasma density, which determines the value of ablation density. The critical density and hence the ablation density in the case of the inverse bremsstrahlung mechanism rise with decreasing the wavelength of laser radiation as $\rho_{cr} \approx \rho_a \propto \lambda^{-2}$. This circumstance is the main reason why the efficiency of laser loading for the third harmonic is far greater than for the first harmonic throughout the 600 – 100 μm laser beam radius range, which corresponds to the inverse bremsstrahlung absorption mechanism for the radiation of both harmonics. The dependences exhibit a maximum, which is caused by the transition from a one-dimensional expansion of the plasma plume to the two-dimensional one with a decrease of laser beam radius and its associated effects of the lowering of ablation density and radiation absorption coefficient.

For the first harmonic radiation, the parameter $I\lambda^2$ increased to 10^{15} W μm^2 cm^{-2} when the laser beam radius was shortened to $R_L = 100$ μm. This signifies that the further shortening of the beam radius in the case of first-harmonic experiments had the effect that the inverse bremsstrahlung mechanism was replaced with the resonance mechanism of radiation absorption. In the case of resonance absorption mechanism, the state of the plasma plume is determined by the fast-electron energy transfer from the region of plasma resonance (the critical-density plasma region), where they are produced, to higher-density material layers. Calculations have shown that the factor of ablation density increase turns out to be stronger than the factor of density lowering that arises from the two-dimensional material expansion. Moreover, the former factor turns out to be so strong that in going over to the resonance absorption mechanism the ablation density begins to increase with shortening the laser beam radius instead of lowering due to the progressively strengthening effect of two-dimensional expansion, as would be the case under the inverse bremsstrahlung mechanism in the absence of fast-electron generation. This rise of ablation density completely accounted for the experimentally measured fraction of the first-harmonic radiation energy transferred to the target as a function of laser beam radius for its small values ($R_L < 100$ μm).

Nevertheless, the results of Ref. [1] had to be regarded merely as an evidence for the manifestation of the effect of fast-electron energy transfer in the ablation rather than a comprehensive investigation of this effect. The point is that the conditions of only one experiment in Ref. [1] (for the beam radius of the first harmonic radiation $R_L = 35$ μm) corresponded completely to the conditions of resonance absorption of laser radiation.

In this connection in the present work we carried out additional experiments under specially selected conditions which correspond to the conversion of absorbed laser energy to the energy of fast electrons.

2. Experimental results

The experiments were performed on the same PALS laser [2] as in Ref. [1], for the same pulse duration and radiation focusing system as well as with the use of similar massive aluminium targets. The following changes were introduced into experimental conditions in comparison with Ref. [1]: only the fundamental harmonic of the iodine laser was used (as a longer-wavelength radiation), the laser pulse energy was substantially increased (up to 360 J), experiments were carried out for a larger set of laser beam radii at the target surface in the range of their relatively small values: $R_L = 35$, 100, 200, 300, 400, and 500 μm. Table 1 presents the calculated values of the radiation intensity I averaged over the pulse duration (assuming the intensity to be uniformly distributed over the beam cross section) and of the parameter $I\lambda^2$ for every shot. These data indicate that

Table 1.

Experimental conditions ($E_L = 360$ J, $\lambda = 1.315$ μm, $\tau = 0.4$ ns)			Experimental data		Calculated values						
$R_L/\mu m$	$I/10^{14}$ W cm^{-2}	$I\lambda^2/10^{14}$ W μm^2 cm^{-2}	$\Omega/10^{-4}$ cm^3	$\eta/10^{-3}$	$\sigma/10^{-2}$	$K_b/10^{-2}$	$K_f/10^{-2}$	E_f/keV	ξ/μm	ρ_a/g cm^{-3}	P_a/Mbar
35	260	450	4.5	6.8	19	–	3.5	25.5	100	0.21	21
100	30	52	2.4	3.6	5.5	–	6.5	8.7	200	0.012	4.8
200	7.5	13	1.7	2.6	2.2	–	12	4.3	330	0.0018	2
300	3.3	5.7	1.6	2.4	–	–	–	–	–	–	–
400	1.9	3.3	1.8	2.7	1.0	27	–	–	316	0.00061	2.4
500	1.2	2.1	2.2	3.5	1.03	33	–	–	284	0.00076	2.5

Notes: R_L is the radius of a laser focal spot on the target; E_L, I, and λ are the radiation energy, intensity, and wavelength, respectively; Ω is the crater volume; η is the efficiency of laser loading; σ is the efficiency of ablative loading; K_b is the absorption coefficient due to the inverse bremsstrahlung; K_f is the laser-to-fast electron energy conversion coefficient; E_f is the energy of a fast electron; ξ is the dimension of a plasma plume; ρ_a is the ablation density; and P_a is the ablative pressure.

the condition $I\lambda^2 > 10^{15}$ W μm^2 cm^{-2} for the resonance absorption of laser radiation in the new series of experiments was fulfilled in three experiments: for $R_L = 35$, 100, and 200 μm.

Like in Ref. [1], investigations were performed with the use of two diagnostic techniques. One technique consisted in the measurement of the dimensions of a crater produced on the target surface and the determination of crater shape. The longitudinal and transverse crater dimensions were measured by optical microscopy techniques. To determine the shape and measure the volume of the crater, target imprints on paraffin were used. The other technique was employed to study the plasma of the vaporised part of the target and involved multiframe interferometric measurements in the plasma of the target material expanding towards the laser beam. In what follows we discuss the crater volume measuring data, which are directly related to the subject of the present work. The shapes of the craters produced in our experiments are depicted in Fig. 1. The crater volumes are given in Table 1, and their dependence on the laser beam radius is plotted in Fig. 2.

The crater is produced due to the phase transition in the target material behind the front of the shock wave generated under the pressure action of the plasma plume, and therefore the crater volume is directly related to the efficiency of laser loading [1, 3]:

$$\Omega = \frac{\eta E_L}{\alpha \varepsilon \rho_0}. \qquad (1)$$

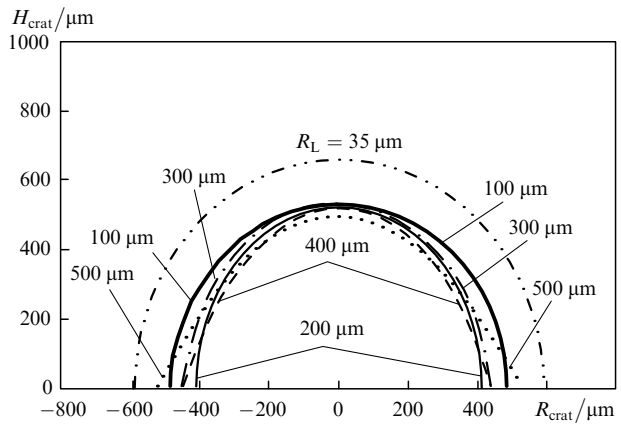

Figure 1. Crater shapes (the depth H_{crat} and the radius R_{crat}) in experiments with different radii of the laser beam R_L.

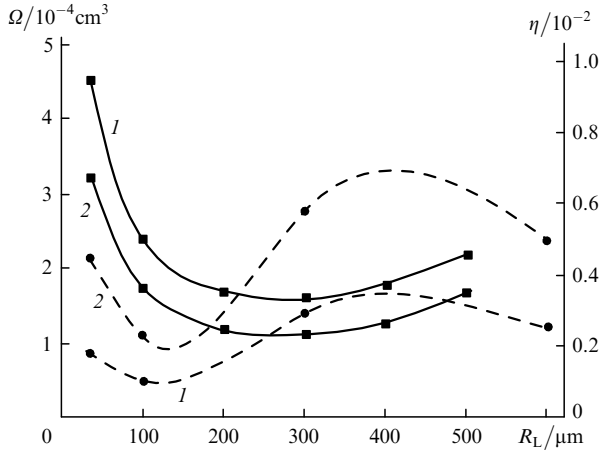

Figure 2. Dependences of the crater volume Ω (*1*) and the efficiency η (*2*) of laser-induced target loading on the laser beam radius R_L obtained experimentally in the present work (solid curves) and in Ref. [1] (dashed curves).

Here, ε is the specific energy required to vaporise a unit mass of material; α is the ratio between the thermal and kinetic energies in the Hugoniot adiabat of the material involved. We resort, like in Ref. [1], to the strong shock wave approximation throughout the course of shock propagation and assume that $\alpha \approx 2$. The value of ε is taken to be equal to 10^3 J g^{-1}, which furnishes good agreement with the experiment according to the numerical calculations of Ref. [4].

The laser loading efficiencies calculated by formula (1) from the experimentally measured crater volumes with the use of the above values of the constants α and ε are collected in Table 1 and shown in Fig. 2. Also shown for comparison in Fig. 2 are the values of the crater volume and the efficiencies of laser loading determined using the fundamental harmonic radiation in the experiments of Ref. [1]. Naturally, the dependences of the laser loading efficiency on the radius reproduce the corresponding dependences for the crater volume.

First of all it is pertinent to note that all the data obtained in the present work belong to that part of the $\eta(R_L)$ dependence which is characterised by the increase in laser loading efficiency with shortening of the laser beam radius after this dependence passes through a minimum. This dependence owes its form to the most interesting processes investigated in the present work: the change of the mechanisms of laser radiation absorption and the two-

dimensional expansion of the plasma plume. As a result of selection of experimental conditions, this part of the $\eta(R_L)$ dependence turned out to be as if 'extended' in comparison with the data of Ref. [1]: it embraces all values of the radius from 35 to 500 μm, while in Ref. [1] only from 35 to 300 μm. Furthermore, only one experimental point (for $R_L = 100$ μm) in Ref. [1] falls in the valley region of the dependence $\eta(R_L)$, to say nothing of its boundaries.

A reliable proof of the growth of laser loading efficiency with decreasing radius of the laser beam in the domain of high $I\lambda^2$ values is the main experimental result of the present work. It is significant that the efficiency growth of laser loading in both series of experiments begins for $I\lambda^2 > 10^{15}$ W μm^2 cm^{-2} (see Fig. 2). In the present work, this value is reached for $R_L = 200$ μm ($I\lambda^2 = 1.3\times 10^{15}$ W μm^2 cm^{-2}); in Ref. [1] it is reached for $R_L = 100$ μm ($I\lambda^2 = 1.4 \times 10^{15}$ W μm^2 cm^{-2}). Moreover, this growth begins for almost equal values of the parameter $I\lambda^2$, to which there correspond close efficiency values of laser loading: 0.0025 in the experiments of the present work and 0.0023 in Ref. [1]. For equal radii of the laser beam, the values of the laser radiation intensity at the target surface and of the parameter $I\lambda^2$ (for the same wavelength) were significantly greater in the present work (by a factor of 3.6). To these higher $I\lambda^2$ values there correspond higher efficiencies of laser loading: for $R_L = 100$ μm, $\eta = 0.0036$ ($I\lambda^2 = 5.2 \times 10^{15}$ W μm^2 cm^{-2}) in comparison with $\eta = 0.0023$ ($I\lambda^2 = 1.4 \times 10^{15}$ W μm^2 cm^{-2}); for $R_L = 35$ μm, $\eta = 0.0068$ ($I\lambda^2 = 4.5 \times 10^{16}$ W μm^2 cm^{-2}) in comparison with $\eta = 0.0045$ ($I\lambda^2 = 1.2 \times 10^{16}$ W μm^2 cm^{-2}).

As shown below, the main cause of all above-listed features of the $\eta(R_L)$ dependence at high laser radiation intensities is the energy transfer by fast electrons.

3. Analysis and interpretation of results

To interpret the experimental data we take advantage of the two-dimensional model of the plasma plume from Ref. [1]. The model was constructed on the basis of approximative matching of the self-similar solutions of the problems on the plane and spherical isothermal expansion of a given material mass [5] involving the introduction of a non-one-dimensionality parameter equal to the ratio between the plume dimension ξ and the laser beam radius R_L. The solutions were obtained for two mechanisms of laser radiation absorption: the inverse bremsstrahlung and the resonance absorption assuming complete conversion of the absorbed energy to the energy of fast electrons. Mathematically, the formulations of the problems for the two absorption mechanisms differed only in the calculation of the plume mass. In the case of inverse bremsstrahlung, the plume mass is defined by the mass flow of the vaporised material with the critical density

$$\rho_{cr} = 1.83 \times 10^{-3} \frac{A}{Z\lambda^2}\,(\text{g cm}^{-3}), \tag{2}$$

and in the case of resonance absorption by the surface mass (the column density) of fast-electron deceleration region. Under the assumption of a monoenergetic spectrum of fast electrons employed in Ref. [1], the deceleration column density is [6]

$$l_0 \approx 1.3 \times 10^{-6}\left(\frac{A}{Z}\right)^2 \frac{E_f^2}{(2+Z)^{1/2}}\,(\text{g cm}^{-2}). \tag{3}$$

In these expressions, E_f is the fast-electron energy in keV; A and Z are the atomic weight of the plasma ions and their average charge.

Given below are the formulas of the model for the calculation of the plasma plume dimension ξ, the plasma plume density ρ_a and pressure P_a at the ablation surface as well as the efficiency of ablative loading of an aluminium target for both absorption mechanisms, which were derived in Ref. [1] with the use of the following constants: the initial target density $\rho_0 = 2.7$ g cm^{-3}, $A = 26$, $Z = 13$ (the substance of the plume was assumed to be completely ionised); the adiabatic exponent of the vaporised part of the target is $\gamma = 5/3$, and the adiabatic exponent for solid aluminium is $\gamma_s = 5/2$. The scaling from Ref. [7]

$$E_f = 1.2(I\lambda^2)^{1/2}\,(\text{keV}) \tag{4}$$

was employed as the formula for the fast-electron energy, in which $I\lambda^2$ is measured in units of 10^{14} W μm^2 cm^{-2}.

1. Inverse bremsstrahlung:

$$\xi = 8.2 \times 10^{-2} K_b^{1/3} I^{1/3} \lambda^{2/3} \tau\,(\text{cm}), \tag{5}$$

$$\rho_a = 2.5\times 10^{-3}\lambda^{-2}\left(1 + 5.85\times 10^{-2} \times \frac{K_b^{1/3} I^{1/3}\lambda^{2/3}\tau}{R_L}\right)^{-2}\,(\text{g cm}^{-3}), \tag{6}$$

$$P_a = 1.35 \times 10^{13} K_{ab}^{2/3} I^{2/3}\lambda^{-2/3} \times\left(1 + 7.4 \times 10^{-2}\frac{K_b^{1/3} I^{1/3}\lambda^{2/3}\tau}{R_L}\right)^{-2}\,(\text{erg cm}^{-3}), \tag{7}$$

$$\sigma = 1.9 \times 10^{-2}\lambda^{-1}\left(1 + 5.23 \times 10^{-2}\frac{K_b^{1/3} I^{1/3}\lambda^{2/3}\tau}{R_L}\right)^{-1}. \tag{8}$$

2. Resonance absorption:

$$\xi = 0.86 K_f^{1/2}\tau^{3/2}\lambda^{-1}\left(1 + 0.8\frac{K_f^{1/2}\tau^{3/2}}{\lambda R_L}\right)^{-1/2}\,(\text{cm}), \tag{9}$$

$$\rho_a = 1.9 \times 10^{-6} I\lambda^3 K_f^{-1/2}\tau^{-3/2}\left(1 + 6.5\frac{K_f^{1/2}\tau^{3/2}}{\lambda R_L}\right)^{1/2}\,(\text{g cm}^{-3}) \tag{10}$$

$$P_a = 5.4\times 10^{11} I\lambda K_f^{1/2}\tau^{-1/2} \times\left(1 + 0.47\frac{K_f^{1/2}\tau^{3/2}}{\lambda R_L}\right)^{-1/2}\,(\text{erg cm}^{-3}), \tag{11}$$

$$\sigma = 6.5 \times 10^{-4} I^{1/2}\lambda^{3/2} K_f^{-1/4}\tau^{-3/4}\left(1 + 9.8\frac{K_f^{1/2}\tau^{3/2}}{\lambda R_L}\right)^{1/4}. \tag{12}$$

Here, K_b is the absorption coefficient in the case of inverse bremsstrahlung; K_f is the laser-to-fast electron energy conversion coefficient (the ratio between the energy of fast electrons and the laser energy) in the case of resonance absorption.

The second terms in the parentheses in expressions (5)–(12) represent the expansion non-one-dimensionality parameter ξ/R_L, multiplied by the matching constant. In the

limiting cases of small and large values of the parameter ξ/R_L, the formulas correspond to the exact self-similar solutions respectively for the plane ($\xi/R_L \ll 1$) and spherical ($\xi/R_L \gg 1$) expansion of the plasma plume. The ablation density and therefore the efficiency of the ablative loading of a one-dimensional plume are determined only by the ratio between the surface mass of the plume and the plume dimension: $\rho_a \propto \sigma^2 \propto l/\xi$. In the case of inverse bremsstrahlung, the ablation density is defined only by the critical plasma density and therefore depends only on the wavelength of laser radiation (as λ^{-2}), in its turn $\sigma \propto \lambda^{-1}$. In the case of resonance absorption mechanism, the surface mass of a one-dimensional plume is a surface mass of the fast-electron deceleration region l_0; furthermore, the dimension of the one-dimensional plume of the self-similar solution depends on l_0 [1]:

$$\xi = \left(\frac{K_f I \tau^3}{l_0}\right)^{1/2}. \qquad (13)$$

In this connection, in view of expression (3), $\rho_a \propto \sigma^2 \propto l_0/\xi \propto I\lambda^3/\tau^{3/2}$.

In going over to the spherical expansion in the case of inverse bremsstrahlung, the ablation density and the efficiency of ablative loading decrease in relation to the increase of the plume volume $\rho_a \propto (\xi/R_L)^{-2}$ and $\sigma \propto \rho_a^{1/2} \propto (\xi/R_L)^{-1}$, while in the case of resonance absorption they decrease much slower: $\rho_a \propto \xi^{-1/2}$ and $\sigma \propto \rho_a^{1/2} \propto \xi^{-1/4}$. The significant effect of the relatively weak effect of two-dimensional expansion on the efficiency of ablative loading in the case of fast-electron energy transfer is attributable to the following fact: with increase in plume surface due to the lateral expansion, the constraint that the surface mass of the plume be constant results in an increase in its total mass and, as a consequence, in a slower density decrease with increase in the plume volume.

The plasma plume parameters and the efficiency of ablative loading were calculated by formulas (9)–(12), which correspond to the resonance absorption mechanism, for the experiments with $R_L = 35$, 100, and 200 μm and by formulas (5)–(8), which correspond to the inverse bremsstrahlung mechanism, for the experiments with $R_L = 400$ and 500 μm. Calculations for the experiment with $R_L = 300$ μm were not performed, because neither of the absorption mechanisms was dominant in the conditions of this experiment. The absorption coefficient K_b and the laser-to-fast electron energy conversion coefficient K_f were determined with the use of formulas (8) and (12) for the efficiency of ablative loading and the use of experimentally determined data for the laser loading efficiency ($K_{b,f} = \eta/\sigma_{b,f}$). The calculated data are collected in Table 1. In addition, Fig. 3 shows the calculated dependences of the ablative pressure, the ablative loading efficiency, and the laser-to-fast electron energy conversion coefficient on the laser beam radius in the 35–200 μm beam radius range, which corresponds to the resonance absorption of laser radiation. Figure 3 also presents the similar dependences from Ref. [1] in the laser beam radius range from 35 to 100 μm.

In the domain of inverse bremsstrahlung, the two-dimensional character of plume expansion is rather strongly manifested even for $R_L = 400$ and 500 μm: the plume dimension ξ is comparable with the laser beam radius (see Table 1). As a result, the ablation density is substantially (by a factor of 2.4–2.6) lower than the critical density ($\rho_{cr} \approx 2 \times 10^{-3}$ g cm^{-3}), the ablative pressure is equal to 2.4–2.5 Mbar, and the efficiency of ablative loading is 0.01. For an insignificant shortening of the laser beam radius (from 500 to 400 μm), the absorption coefficient changes only slightly, from 0.33 to 0.27. However, it is precisely this circumstance that is the main factor responsible for the lowering of laser loading efficiency from 3.5×10^{-3} to 2.7×10^{-3}.

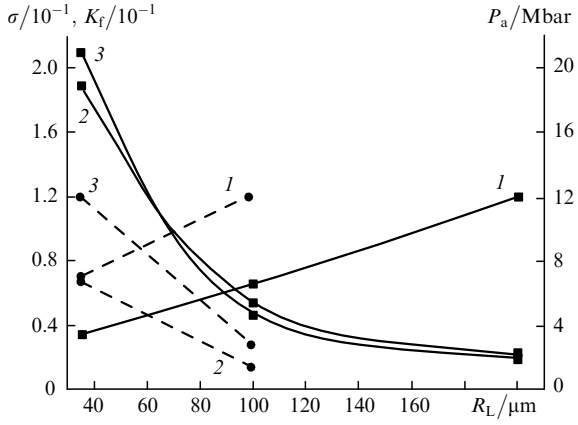

Figure 3. Dependences of the laser-to-fast electron energy conversion coefficient K_f (*1*), the efficiency of ablative loading σ (*2*), and the ablative pressure P_a (*3*) on the laser beam radius R_L calculated assuming the experimental conditions of the present work (solid curves) and Ref. [1] (dashed curves).

In the resonance absorption domain in the range $R_L = 200 - 35$ μm, the two-dimensional character of plume expansion becomes much more pronounced. For $R_L = 200$ μm the plume dimension exceeds the radius of the laser spot by a factor of 1.65, for $R_L = 35$ μm almost by a factor of 3 (see Table 1). However, the energy transfer by fast electrons exerts a substantially stronger effect on the state of the plasma plume than the two-dimensional expansion. As a result, the ablation density, the ablative pressure, and the ablative loading efficiency increase rapidly in this domain with a decrease in laser beam radius and the corresponding increase in the radiation intensity (see Table 1 and Fig. 3), because this leads to a growth of the fast-electron energy [$E_f \propto I^{1/2} \propto R_L^{-1}$, see formula (4)] and the consequential increase in their penetration depth in the plasma [$l_0 \propto E_f^2 \propto I \propto R_L^{-2}$, see formula (3)].

The ablative pressure increases from 2 Mbar for $R_L = 200$ μm, when the fast-electron energy is $E_f \approx 4.3$ keV, to 21 Mbar for $R_L = 35$ μm, when the fast-electron energy amounts to 25.5 keV. In this case, the efficiency of ablative loading rises from 0.022 to 0.19 and the laser-to-fast electron energy conversion coefficient decreases from 0.12 to 0.035. As a result, the rise in laser loading efficiency with decreasing the laser beam radius turns out to be weaker than the growth of ablative loading efficiency and nevertheless significant: from 2.6×10^{-3} for $R_L = 200$ μm to 6.8×10^{-3} for $R_L = 35$ μm.

A comparison with the data of Ref. [1] (see Fig. 3) shows that a 3.6-fold rise in the laser beam intensity, all other factors being the same, results in an almost two-fold increase in the ablative pressure, a three-four-fold rise in the ablative loading efficiency, a 1.5-fold rise in the efficiency of laser loading, and a two-fold decrease in the laser-to-fast

electron energy conversion coefficient. In the context of the present work we can do no more than hypothesise about the cause of this decrease, because the conversion coefficient is the only unknown in our problem which was not measured in the experiment and not calculated within the framework of our theoretical model. Instead, this unknown was defined as a coefficient from the comparison of experimental and theoretical data. This decrease is supposedly due to the properties of the resonance absorption of laser radiation, specifically, to the dependence of the efficiency of resonance absorption on the angle between the direction of laser radiation propagation and the direction of plasma density gradient. For the same radius of the laser beam, the higher radiation intensity under the experimental conditions of the present work results in the stronger effects of ponderomotive pressure and two-dimensional material expansion than in Ref. [1]. This in its turn may be responsible for the formation of a spatial plasma density distribution near the critical-density region such that the set of angles of laser radiation incidence on the plasma corresponds to a smaller coefficient of resonance absorption and, as a consequence, to a smaller laser-to-fast electron energy conversion coefficient.

4. Conclusions

The results of experimental and theoretical investigations outlined in this work allow the conclusion about the decisive role of fast-electron energy transfer during energy transfer from the laser pulse to the non-vaporised part of the target under the resonance mechanism of radiation absorption. The heating of dense material layers by fast electrons is responsible for the production of a plasma plume with an ablation density which far exceeds the critical density, resulting in an efficient energy transfer from the laser plume to the shock wave propagating through the solid part of the target. As the laser pulse intensity increases, the fraction of laser plume energy transferred to the shock wave increases, because increasing the intensity increases the energy of fast electrons and, as a consequence, their penetration depth in the target material. As a result, despite the decrease in the laser-to-fast electron energy conversion coefficient and the strongly pronounced two-dimensional character of the expansion of the plasma plume, in experiments involving aluminium target irradiation by the first harmonic of iodine laser radiation we recorded a significant (by more than a factor of 2.5) increase in the energy fraction of the laser pulse transferred to the shock wave with increasing the intensity from 7.5×10^{14} to 2.6×10^{16} W cm^{-2}.

Therefore, the results of the present work supplement those of Ref. [1] and bear out the theoretical conclusions [6, 7] about the feasibility of producing high ablative pressure and transferring a significant energy fraction of the laser pulse to the non-vaporised part of the target due to the energy transfer by fast electrons in the target irradiation by relatively long-wavelength laser radiation

Acknowledgements. This work was partly supported by the Russian Foundation for Basic Research (Grant Nos 05-01-00631 and 05-02-16856), the EUROATOM-IPPLM Association (Contract No. FU06-CT-2004-00081), the Polish Ministry of Science and Information Technology (Project No. 3 T10B 024 273), and the Ministry of Education, Youth and Sports of the Czech Republic (Project No. LC528).

References

1. Gus'kov S.Yu., Borodziuk S., Kalal M., et al. *Kvantovaya Elektron.*, **34** (11), 989 (2004) [*Quantum Electron.*, **34** (11), 989 (2004)].
2. Jungwirth K., Cejnarova A., Juha L., et al. *Phys. Plasmas*, **8**, 2495 (2001).
3. Gus'kov K.S., Gus'kov S.Yu. *Kvantovaya Elektron.*, **31** (4), 305 (2001) [*Quantum Electron.*, **31** (4), 305 (2001)].
4. Afanasiev Yu.V., Chichkov B.N., Demchenko N.N., et al. *J. Rus. Laser Res.*, **20**, 89 (1999).
5. Imshennik V.S. *Dokl. Akad. Nauk SSSR*, **5**, 263 (1960).
6. Afanas'ev Yu.V., Gus'kov S.Yu., in *Nuclear Fusion by Inertial Confinement*. Ed. by G. Velarde et al. (Ann Arbor: CRC Press, 1993) pp 99–118.
7. Gus'kov S.Yu., Zverev V.V., Rozanov V.B. *Kvantovaya Elektron.*, **10** (4), 802 (1983) [*Sov. J. Quantum Electron.*, **13** (4), 498 (1983)].